View metadata, citation and similar papers at core.ac.uk

brought to you by CORE

provided by Drexel Libraries E-Repository and Archives

Drexel University
Libraries

Drexel E-Repository and Archive (iDEA)
http://idea.library.drexel.edu/

Drexel University Libraries
www.library.drexel.edu

The following item is made available as a courtesy to scholars by the author(s) and Drexel University Libraries and may contain materials and content, including computer code and tags, artwork, text, graphics, images, and illustrations (Material) which may be protected by copyright law. Unless otherwise noted, the Material is made available for nonprofit and educational purposes, such as research, teaching and private study. For these limited purposes, you may reproduce (print, download or make copies) the Material without prior permission. All copies must include any copyright notice originally included with the Material. **You must seek permission from the authors or copyright owners for all uses that are not allowed by fair use and other provisions of the U.S. Copyright Law.** The responsibility for making an independent legal assessment and securing any necessary permission rests with persons desiring to reproduce or use the Material.

Please direct questions to archives@drexel.edu

AIP | Journal of Applied Physics

Optimum cavity length for high conversion efficiency quantum well diode lasers

D. P. Bour and A. Rosen

Citation: J. Appl. Phys. 66, 2813 (1989); doi: 10.1063/1.344209
View online: http://dx.doi.org/10.1063/1.344209
View Table of Contents: http://jap.aip.org/resource/1/JAPIAU/v66/i7
Published by the American Institute of Physics.

Related Articles

Modeling light absorption by bound electrons in self-assembled quantum dots
J. Appl. Phys. 113, 083101 (2013)

A modular optically powered floating high voltage generator
Rev. Sci. Instrum. 84, 024701 (2013)

Numerical simulation of organic semiconductor devices with high carrier densities
J. Appl. Phys. 112, 114909 (2012)

A low-noise large dynamic-range readout suitable for laser spectroscopy with photodiodes
Rev. Sci. Instrum. 83, 104704 (2012)

Study of asymmetries of Cd(Zn)Te devices investigated using photo-induced current transient spectroscopy, Rutherford backscattering, surface photo-voltage spectroscopy, and gamma ray spectroscopies
J. Appl. Phys. 112, 074503 (2012)

Additional information on J. Appl. Phys.

Journal Homepage: http://jap.aip.org/
Journal Information: http://jap.aip.org/about/about_the_journal
Top downloads: http://jap.aip.org/features/most_downloaded
Information for Authors: http://jap.aip.org/authors

ADVERTISEMENT

Downloaded 13 Mar 2013 to 129.25.131.13. Redistribution subject to AIP license or copyright; see http://jap.aip.org/about/rights_and_permissions

Optimum cavity length for high conversion efficiency quantum well diode lasers

D. P. Bour and A. Rosen
David Sarnoff Research Center, CN 5300, Princeton, New Jersey 08543-5300

(Received 3 March 1989; accepted for publication 16 May 1989)

The cavity length which maximizes the peak power conversion efficiency is determined for quantum well diode lasers. These calculations are based upon simple models of the diode injection laser's electrical and optical behaviors, including saturation in the quantum well gain-current characteristic. Here the influences of the distributed optical cavity loss, electrical resistivity, and facet reflectivity on the optimum cavity length are described. Although a lower facet reflectivity results in increased threshold current, there are advantages to longer devices, as the peak conversion efficiency is not reduced. Since the optimum cavity length is greater for low reflectivity, the diode series resistance is smaller. Furthermore, when operating at the point where conversion efficiency is a maximum, the power output of the device with low facet reflectivity exceeds that of the device with higher facet reflectivity. Therein lies the principle advantage of reduced front-facet reflectivities in high power, high efficiency quantum well diode lasers. Good agreement results when these predictions are applied to a strained InGaAs/AlGaAs single quantum well laser ($\lambda = 0.93\ \mu$m).

I. INTRODUCTION

Among the current applications of incoherent, high-power AlGaAs diode laser arrays are optical triggering of *p-i-n* diodes,[1] and optical pumping of Nd^{3+} ions in various host crystals.[2] For such applications, it is desirable to not only have high power output, but high power conversion efficiency as well, so that heat-sinking requirements are minimized. Thus, quantum well (QW) diode lasers have proven most appropriate, due to their low threshold currents; to date QW devices have been reported with conversion efficiencies exceeding 57%.[3] A simple model of the QW laser diode's optical and electrical behavior demonstrates that conversion efficiencies are low in the short-cavity regime, due primarily to the high threshold current of short-cavity QW lasers. Similarly, in long-cavity lasers the reduced external quantum efficiencies along with increasing threshold current also lead to poor conversion efficiencies. Here we apply recently developed theories[4,5] concerning the gain-current relationship in QW lasers to determine the optimum cavity length for high conversion efficiency QW diode lasers.

II. CONVERSION EFFICIENCY

Above threshold, the light output (P_{out}) versus drive current (I) characteristic is a simple linear relation[6]:

$$P_{out}(I) = \eta_e\ (h\nu/q)(I - I_{th}), \quad (1)$$

where $h\nu$ is equal to the photon energy, q is the electronic charge, η_e is the external differential quantum efficiency (DQE), and I_{th} is the threshold current. Similarly, for currents well above the diode turn-on voltage (V_0), the diode voltage (V) increases linearly with drive current[6]:

$$V(I) = V_0 + IR_s, \quad (2)$$

where R_s is the series resistance of the the diode. The drive power is equal to the current-voltage (I-V) product.

Often it is assumed that $V_0 = h\nu/q$. Although the diode begins to pass current when $V > h\nu/q$, a realistic diode I-V characteristic demonstrates a turn-on region spanning several tenths of a volt. Therefore, we do not require that $V_0 = h\nu/q$, and instead assume a value $V_0 > h\nu/q$. In an extrapolation of the I-V characteristic from the high-current regime (where it is approximately linear) back to $I = 0$, we normally find for our AlGaAs QW diode lasers (with $h\nu \sim 1.5$ eV) that $V_0 \sim 1.9$ V. We note that this value is slightly lower than the band-gap energy of the cladding layers. Thus, diode voltage can be underestimated if we set $V_0 = h\nu/q$, but by allowing V_0 to be greater than $h\nu/q$ a better fit to the measured diode I-V characteristic is obtained, especially for high-drive currents. A realistic range of V_0 values is $1.5\ \text{V} < V_0 < 2.2\ \text{V}$, where the lower limit is the photon energy, and the upper limit is determined by the band gap of the cladding layers.

The power conversion efficiency (η_c) as a function of drive current is

$$\eta_c(I) = \eta_e(h\nu/q)[(I - I_{th})/I(V_0 + IR_s)]. \quad (3)$$

The condition $d\eta_c/dI = 0$ determines the current at which the conversion efficiency is maximum (I_0):

$$I_0 = I_{th}(1 + \sqrt{1 + x}), \quad (4)$$

where x is a dimensionless parameter defined as $x = V_0/I_{th}R_s$. Consequently, the peak conversion efficiency is

$$\eta_c^{peak} = \eta_c(I_0) = \eta_e(h\nu/qV_0)[x/(1 + \sqrt{1 + x})^2], \quad (5)$$

while the power output at the point of peak conversion efficiency is

$$P_0 = P_{out}(I_0) = \eta_e(h\nu/q)I_{th}\sqrt{1 + x}. \quad (6)$$

We seek to maximize the peak conversion efficiency, while concurrently producing a high power output at the η_c^{peak} operating point.

Downloaded 13 Mar 2013 to 129.25.131.13. Redistribution subject to AIP license or copyright; see http://jap.aip.org/about/rights_and_permissions

III. CAVITY LENGTH DEPENDENCE

Since the quantities η_e, R_s, and I_{th} are dependent upon the cavity length (L), the cavity length may be chosen to maximize the peak conversion efficiency; the optimum cavity length is that which maximizes η_c^{peak}. The cavity-length dependence of the threshold current is especially strong in QW lasers, where I_{th} increases sharply in short-cavity devices, due to high average losses along with QW gain saturation.[4,5,7] The modal gain at threshold is $G_{th} = \alpha + (1/2L)\ln(1/R_f R_r)$, where α is the distributed optical loss (consisting of absorption and scattering losses), and R_f and R_r are the front- and rear-facet power reflectivities, respectively (R_r is taken to be 1 since the highest front-end power is desirable). Recent modeling of QW laser diodes by Chinn, Zory, and Reisinger[4] has shown that the modal gain (G) increases logarithmically with drive current density (J), or $G = G_0 \ln(J/J_0)$. Although the parameters G_0 and J_0 are structure and temperature dependent, values $G_0 \cong 40$ cm^{-1} and $J_0 \cong 100$ A/cm^2 were shown to closely reproduce the rigorously calculated gain-current relationship for a typical QW laser structure. Likewise, these values predict threshold currents which are in very good agreement with experimental results, and so are retained here for illustrative calculations. For instance, a threshold current density of $J_{th} = 240$ A/cm^2 results for a diode with uncoated facets ($R = 0.3$), $\alpha = 5$ cm^{-1} and $L = 400\,\mu$m. The cavity-length dependence of threshold current is given by

$$I_{th}(L) = J_0 WL \exp \frac{1}{G_0}\left(\alpha + \frac{1}{2L}\ln\frac{1}{R_f R_r}\right), \qquad (7)$$

where W is the stripe width.

The external DQE is also cavity length dependent, as the presence of any internal optical loss reduces η_e below the internal DQE (η_i)[8]:

$$\frac{1}{\eta_e(L)} = \frac{1}{\eta_i}\,[\alpha + (1/2L)\ln(1/R_f R_R)]/ (1/2L)\ln(1/R_f R_r)\,. \qquad (8)$$

Although the internal DQE does not influence the calculated optimum cavity length, both η_c^{peak} and P_0 are directly proportional to η_i.

The final quantity which depends on cavity length is the diode series resistance, which is inversely proportional to the stripe area, and so increases in short-cavity devices:

$$R_s(L) = \rho_s / WL\,. \qquad (9)$$

Here ρ_s is the sheet resistivity, including contributions from both material resistivity and contact resistivity. Low values of ρ_s are desirable to reduce the voltage drop across the diode, thereby reducing heating and power consumption. Sheet resistivities as low as $\rho_s = 1\times 10^{-4}\ \Omega$ cm^2 have been achieved.[3] This is equivalent, for example, to a series resistance $R_s = 0.5\ \Omega$ for a $50\times 400\ \mu$m^2 stripe laser. A lower limit to ρ_s is $\sim 1\times 10^{-5}\ \Omega$ cm^2, based upon the hole transport properties of the heavily doped AlGaAs P-cladding layer.

Combining Eqs. (5) and (7)–(9) gives the cavity-length dependence of peak conversion efficiency, as shown in Fig. 1. Parameters used are typical of high-performance QW laser material: $G_0 = 40$ cm^{-1}, $J_0 = 100$ A/cm^2, $V_0 = 1.9$ V, $\rho_s = 1\times 10^{-4}\ \Omega$ cm^2, $\alpha = 5$ cm^{-1}, $h\nu = 1.5$ eV, and $\eta_i = 0.9$. Rear-facet reflectivity is $R_r = 1.0$, while the calculated $\eta_c^{peak}(L)$ result is shown for two front-facet reflectivities, $R_f = 0.1$ and $R_f = 0.3$. Comparing these curves shows that the facet reflectivity does not affect the maximum value of peak conversion efficiency; for the parameters used here the maximum η_c^{peak} is ~ 0.49 for each case. Furthermore, the optimum cavity length (L_o, the cavity length where η_c^{peak} is maximum) is shorter for the case of higher reflectivity. Additionally, η_c^{peak} is a more sensitive function of cavity length when the reflectivity is high.

IV. OPTIMUM CAVITY LENGTH

For short-cavity QW lasers, threshold current and series resistance are great, so that η_c^{peak} is low. Similarly, in the long-cavity regime, although threshold current densities and series resistances are low, the internal optical losses lead to a low external DQE, thereby reducing η_c^{peak}. In addition, as threshold current densities are only slowly decreasing in the long-cavity regime, at some point the threshold current begins to increase with cavity length; I_{th} is minimum when $L = (1/2G_0)\ln(1/R_f R_r)$. Thus at each extreme the conversion efficiency is low, and the goal here is to adjust cavity length so that η_c^{peak} is greatest. Setting $d\eta_c^{peak}/dL = 0$ is the condition for maximizing η_c^{peak} with respect to cavity length; the resultant equality determining the optimum cavity length (L_o) is

$$1 + (xy/z\eta_e)\sqrt{1+x} = 0, \qquad (10)$$

where y and z are defined as

$$y \equiv \frac{d\eta_e}{dL} = \frac{-(\alpha\eta_e/L)}{\alpha + (1/2L)\ln(1/R_f R_r)}, \qquad (11a)$$

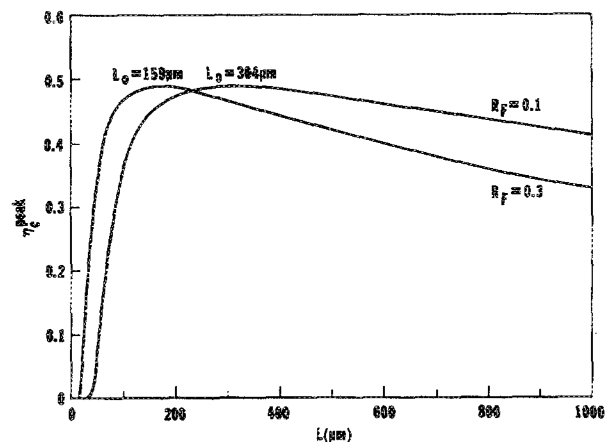

FIG. 1. Cavity length (L) dependence of peak power conversion efficiency (η_c^{peak}), for the case of rear-facet reflectivity $R_r = 1$ and front-facet reflectivities $R_f = 0.3$ and $= 0.1$ ($G_0 = 40$ cm^{-1}, $J_0 = 100$ A/cm^2, $V_0 = 1.9$ V, $\rho_s = 1\times 10^{-4}\ \Omega$ cm^2, $\alpha = 5$ cm^{-1}, $h\nu = 1.5$ eV, and $\eta_i = 0.9$).

Downloaded 13 Mar 2013 to 129.25.131.13. Redistribution subject to AIP license or copyright; see http://jap.aip.org/about/rights_and_permissions

$$z \equiv \frac{dx}{dL} = \frac{x}{G_0 L} (1/2L)\ln(1/R_f R_r) . \quad (11b)$$

Note that Eq. (10) is ultimately independent of both W and η_i, so these parameters have no effect on L_o.

The solution of Eq. (10) gives the optimum cavity length, and is useful in determining how various parameters affect L_o. In addition to the gain parameters G_0 and J_0, the most important material characteristics influencing L_o are the sheet resistivity ρ_s (because it determines how the diode power consumption increases with drive current) and the internal optical loss α (since given some internal quantum efficiency, optical losses place the fundamental limit on the diode power output). Thus, Fig. 2 shows contours of constant L_o, plotted as a function of α and the dimensionless quantity $(V_0 / J_0 \rho_s)$. From these contours, L_o's sensitivity to variations in α, V_0, J_0, and ρ_s can be seen; and in order to illustrate the effect of G_0, calculations for $G_0 = 40$ cm^{-1} (solid curves) and $G_0 = 35$ cm^{-1} (dashed curves) are shown. Facet reflectivities are $R_r = 1$ and $R_f = 0.3$. Note that for low optical losses, long cavities are desirable. In this case, threshold current densities are lower and external quantum efficiencies are still high relative to the case of higher optical loss. Similarly, in the case of high sheet resistivity it is advantageous to have long cavities, since increased diode area reduces the series resistance. Although L_o is influenced by many factors, it is important to note that all parameters can be obtained by characterizing simple, broad-area lasers.

V. EFFECT OF FACET REFLECTIVITY

Figure 2 shows how the internal optical loss, the gain, and the electrical characteristics determine the optimum cavity length for $R_r = 1$ and $R_f = 0.3$. The facet reflectivity is a fabrication parameter which also plays a strong role through its effect on threshold current [Eq. (7)] and external DQE [Eq. (8)]. While the front-facet coating is typically a single-layer dielectric (Al_2O_3) film of appropriate thickness to give $0 < R_f < 0.3$, the rear-facet coating is a stack of $\lambda/4$ dielectric layers to achieve high reflectivity. Referring to the condition determining L_o [Eq. (10)], it is important to notice that the cavity length always appears in a term $(1/2L)\ln(1/R_f R_r)$. Therefore, if the facet reflectivity is changed while all other parameters remain constant, the quantity $(1/2L_o)\ln(1/R_f R_r)$ must not change if the equality in Eq. (10) is to be maintained. Subsequently, the result of changing the front-facet reflectivity from R_f to R_f' is a change in the optimum cavity length from its old value L_o to a new value L_o':

$$L_o' = L_o \frac{\ln(1/R_f' R_r)}{\ln(1/R_f R_r)} . \quad (12)$$

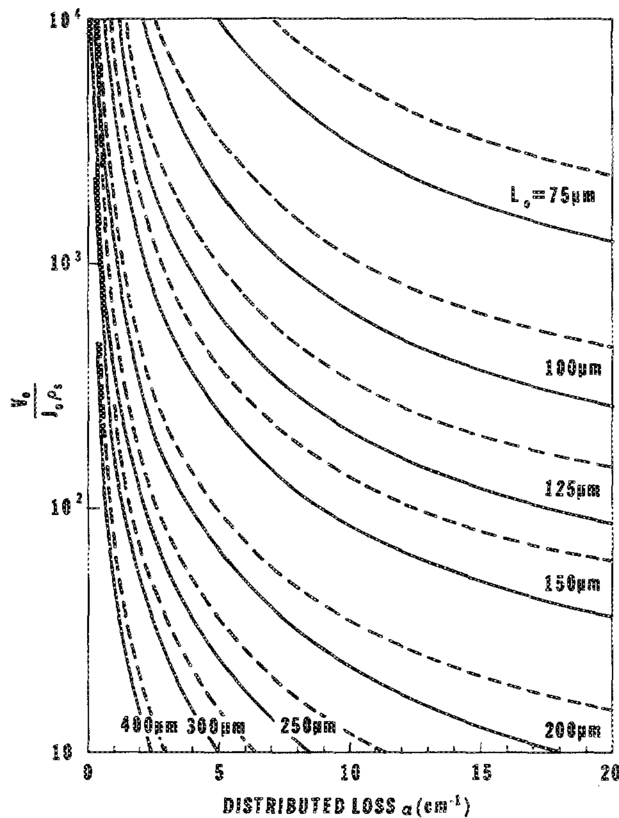

FIG. 2. Curves of constant L_o (optimum cavity length); dependence on the internal optical loss (α) and the dimensionless parameter $(V_0/J_0\rho_s)$, calculated for $R_r = 1$ and $R_f = 0.3$. Solid curves are for $G_0 = 40$ cm^{-1}, dashed curves for $G_0 = 35$ cm^{-1}. If the front-facet reflectivity is changed to a new value R_f', the value of each L_o contour should be multiplied by $\ln[(1/R_f')]/\ln[(1/0.3)]$.

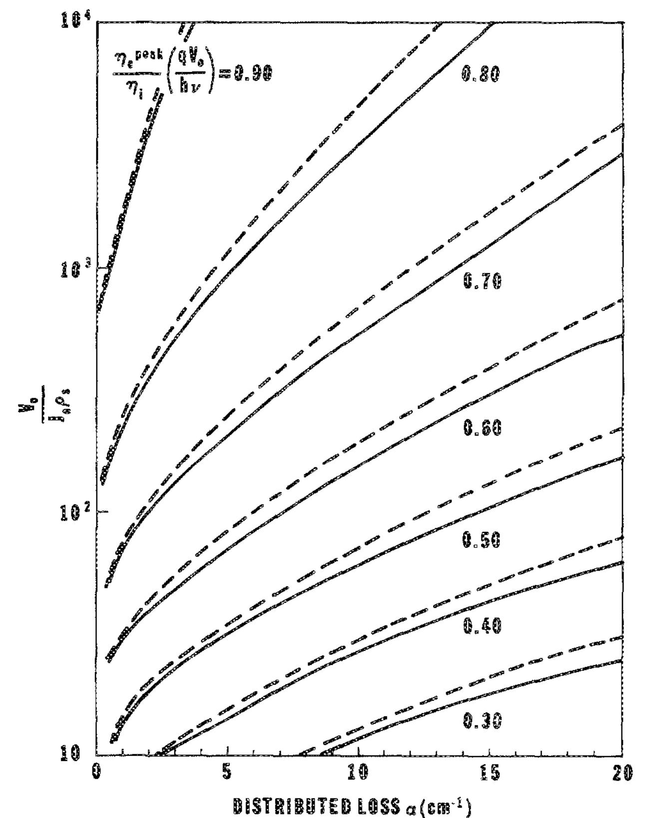

FIG. 3. Contours where normalized peak conversion efficiency $(\eta_c^{peak}/\eta_i)(qV_0/h\nu)$ is constant: optical loss (α) and $(V_0/J_0\rho_s)$ dependence. Solid curves are for $G_0 = 40$ cm^{-1}, dashed curves for $G_0 = 35$ cm^{-1}.

Downloaded 13 Mar 2013 to 129.25.131.13. Redistribution subject to AIP license or copyright; see http://jap.aip.org/about/rights_and_permissions

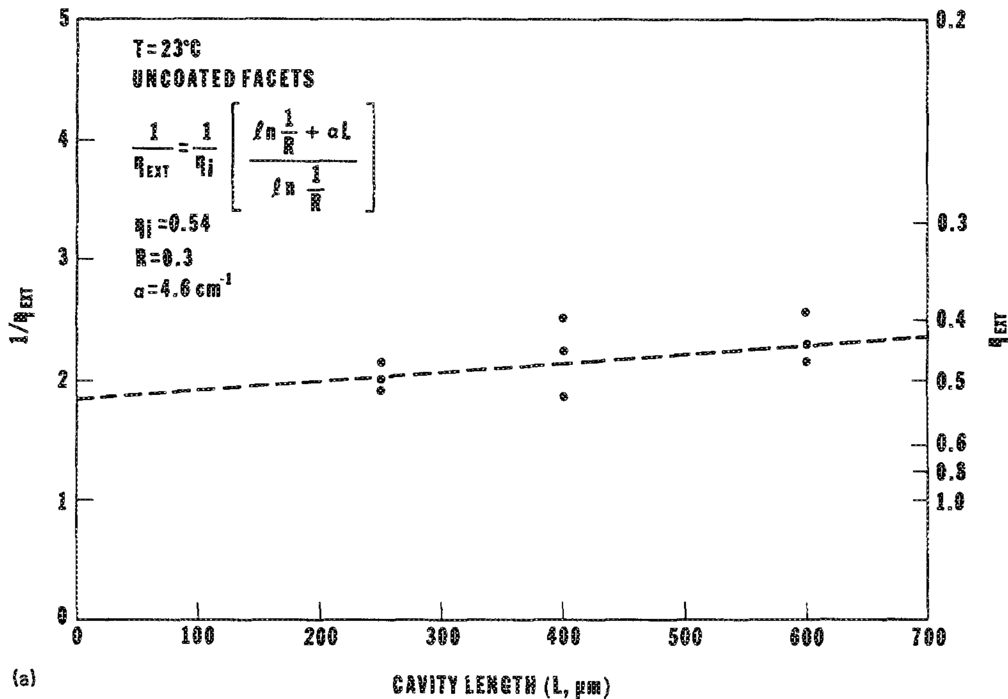

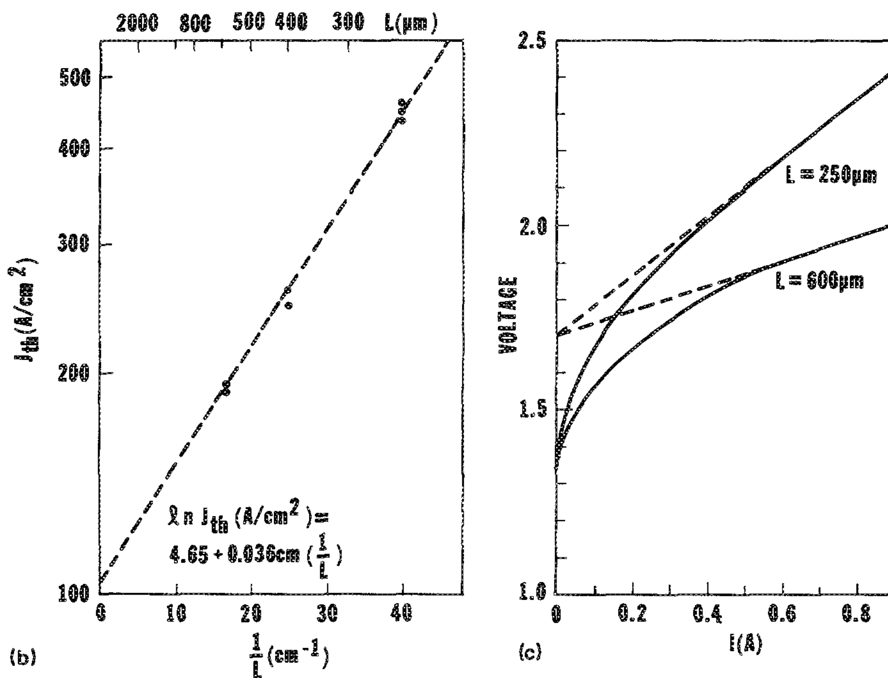

FIG. 4. Characteristics of strained InGaAs/AlGaAs single-quantum well laser: (a) plot of $1/\eta_e$ vs L and linear fit used to determine $\eta_i = 0.54$ and $\alpha = 4.6$ cm^{-1}; (b) plot of $\ln(J_{th})$ vs $(1/L)$ and linear fit used to determine $G_0 = 33.4$ cm^{-1}, $J_0 = 91.1$ A/cm^2; and (c) current-voltage characteristic of diodes with $L = 250$ and $L = 600$ μm ($W = 90$ μm), along with linear fits using $V_0 = 1.7$ V and $\rho_s = 1.8 \times 10^{-4}$ Ω cm^2.

This is demonstrated in Fig. 1, where L_o is increased from 159 to 304 μm when the front-facet reflectivity is reduced from $R_f = 0.3$ to 0.1 ($R_r = 1$). Likewise, the constant L_o contours of Fig. 2 may be appropriately rescaled according to Eq. (12) if the reflectivity is changed. For example, if the front-facet reflectivity is reduced from $R_f = 0.3$ to 0.1, each contour's L_o value increases by a factor of ~ 1.9.

Since the quantity $(1/2L_o)\ln(1/R_f R_r)$ is unchanged when the facet reflectivity is altered, neither the external DQE [Eq. (8)] nor the peak conversion efficiency [Eq. (5)] of optimized devices are affected by such changes, as is evidenced by Fig. 1. For devices with optimum cavity length, contours of constant normalized peak conversion efficiency $(\eta_c^{\rm peak}/\eta_i)(qV_0/h\nu)$, dependent upon the cavity optical loss α and the dimensionless quantity $(V_0/J_0\rho_s)$, are shown in Fig. 3. As in Fig. 2, the solid curves are for $G_0 = 40$ cm^{-1} while the dashed curves are for $G_0 = 35$ cm^{-1}. These contours are not affected by facet reflectivity, and they demonstrate how low optical loss and low sheet resistivity both contribute to a high peak conversion efficiency. For high

Downloaded 13 Mar 2013 to 129.25.131.13. Redistribution subject to AIP license or copyright; see http://jap.aip.org/about/rights_and_permissions

performance laser material, Fig. 3 predicts $\eta_c^{\rm peak} \geqslant 0.5$, in agreement with the best observed conversion efficiencies.[2,3]

Although the attainable $\eta_c^{\rm peak}$ is unaffected by facet reflectivity, the power output at the $\eta_c^{\rm peak}$ operating point [P_0, Eq. (6)] is increased for optimized diodes with reduced reflectivities. In fact, both the threshold current and P_0 are changed by the same factor as the optimum cavity length itself. For example, if the front-facet reflectivity were reduced from $R_f = 0.3$ to 0.1, L_o, $I_{\rm th}$, and the corresponding P_0 would increase by a factor ~ 1.9. Therein lies the primary advantage of low front-facet reflectivities in high-power diode arrays. Although threshold currents are increased, in optimized devices the power output is greater at the operating condition of peak conversion efficiency. Moreover, since longer cavities are optimal in the situation of low R_f, diode series resistance is also reduced. The front-facet reflectivity is more sensitive to facet-coating thickness fluctuations when $R_f = 0.1$, however, than when $R_f = 0.3$ (thickness $= \lambda/2$).

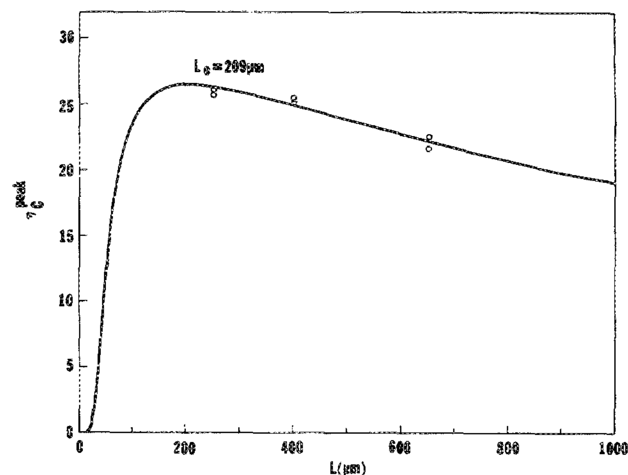

FIG. 5. Solid line: predicted peak conversion efficiency as a function of cavity length for strained InGaAs/AlGaAs laser with $R_r = 1$, $R_f = 0.3$; open circles: measured peak conversion efficiencies for devices with highly reflective rear-facet coating and $\lambda/2$ front-facet coating ($R_f = 0.3$).

VI. COMPARISON WITH EXPERIMENT

These optimization calculations have been applied to a strained InGaAs/AlGaAs single-quantum-well (SQW) laser. The laser structure is similar to low threshold GaAs/AlGaAs SQW lasers, and consists of a 70-Å strained $In_{0.2}Ga_{0.8}As/Al_{0.2}Ga_{0.8}As$ SQW with $Al_xGa_{1-x}As (0.2 < x < 0.6)$ graded-index separate confinement heterostructure, grown by atmospheric pressure organometallic vapor phase epitaxy.[9] For a strained QW, lasing wavelength depends not only on alloy composition and quantum shifts, but also on the strain-induced band gap shift.[10] Here a biaxial compression increases the band gap, resulting in a lasing wavelength $\lambda = 0.93$ μm ($h\nu = 1.33$ eV). Simple broad-area lasers (90-μm-wide oxide stripe) of several cavity lengths, and with uncoated facets, were used to determine the appropriate parameters (G_0, J_0, V_0, α, η_i, and ρ_s).

Shown in Fig. 4(a) as a function of cavity length are the observed values of the inverse external DQE ($1/\eta_e$, solid points). Fitting to the linear behavior predicted by Eq. (8) (dashed line), the internal quantum efficiency and internal optical losses are found to be $\eta_i = 0.54$ and $\alpha = 4.6$ cm^{-1}, respectively. In a similar manner, the threshold current density ($J_{\rm th} = I_{\rm th}/WL$) depends on cavity length through Eq. (7). A linear fit of $\ln(J_{\rm th})$ to $1/L$ (dashed line) fits the measured threshold current densities (solid points) as shown in Fig. 4(b). The gain parameters thus obtained from this fit and the previously obtained optical loss are $G_0 = 33.4$ cm^{-1} and $J_0 = 91.1$ A/cm^2. The current-voltage characteristic of both a 90×250 μm^2 laser and a 90×600 μm^2 laser are shown by the solid curves in Fig. 4(c). These curves are well approximated (dashed lines) by using $V_0 = 1.7$ V and $\rho_s = 1.8 \times 10^{-4}$ Ω cm^2 in Eqs. (2) and (9).

The parameters obtained in this way ($V_0 = 1.7$ V, $\rho_s = 1.8 \times 10^{-4}$ Ω cm^2, $G_0 = 33.4$ cm^{-1}, $J_0 = 91.1$ A/cm^2, $\alpha = 4.6$ cm^{-1}, and $\eta_i = 0.54$) are used to predict the optimum cavity length for a high conversion efficiency, strained SQW laser with facet coatings. For rear-facet reflectivity $R_r = 1$ and front-facet reflectivity $R_f = 0.3$, Fig. 5 shows the expected cavity-length dependence of peak power conversion efficiency for lasers fabricated from this material. The maximum attainable conversion efficiency is $\eta_c^{\rm peak} \sim 26\%$, at the optimum cavity length $L_o = 209$ μm.

To compare with these predictions, broad-area oxide-stripe lasers of various cavity lengths and with highly reflective dielectric stack coatings on the rear facet ($R_r > 0.95$) and a $\lambda/2$ Al_2O_3 coating ($R_f = 0.3$) on the front facet were fabricated from this material and tested. Measured peak conversion efficiencies (open circles) agree well with the prediction, as shown in Fig. 5, thereby illustrating the tendency toward an optimum cavity length. Thus, the strained-layer laser behavior is accurately described by these simple models. Moreover, by fully characterizing the laser material using simply fabricated lasers with uncoated facets, the optimum cavity length of more useful devices (with coated facets) has been obtained.

VII. SUMMARY

Simple models of diode laser optical and electrical behavior, used in conjunction with a realistic description of the QW gain-current relationship, predict the optimum cavity length for high-power conversion efficiency QW lasers. We have specifically determined how the optimum cavity length is influenced by the gain, loss, facet reflectivity, and electrical characteristics. Reducing the front-facet reflectivity results in higher threshold current, and requires that optimized devices be made longer. It does not affect the maximum attainable conversion efficiency, however, and offers the advantage of lower series resistance and a higher-power output at the point of peak conversion efficiency. These results were applied to a strained InGaAs/AlGaAs strained quantum well laser; and they can be applied to other QW laser structures using the appropriate parameters, all of which can be measured on broad-area lasers.

Downloaded 13 Mar 2013 to 129.25.131.13. Redistribution subject to AIP license or copyright; see http://jap.aip.org/about/rights_and_permissions

ACKNOWLEDGMENTS

The authors thank G. A. Evans, N. W. Carlson, P. Stabile, S. Palfrey, D. B. Carlin, L. Elbaum, J. C. Connolly, and M. Ettenberg of the David Sarnoff Research Center for useful discussions and encouragement.

[1]A. Rosen, P. J. Stabile, D. W. Bechtle, W. Janton, A. M. Gombar, J. McShea, A. Rosenberg, P. W. Herczfeld, and A. Bahasadri, IEEE Trans. Electron Devices **ED-36**, 367 (1989).

[2]W. Streifer, D. R. Scifres, G. L. Harnagel, D. F. Welch, J. Berger, and M. Sakamoto, IEEE J. Quantum Electron. **QE-24**, 883 (1988).

[3]R. G. Waters, D. K. Wagner, D. S. Hill, P. L. Tihanyi, and B. J. Vollmer, Appl. Phys. Lett. **51**, 1318 (1987).

[4]S. R. Chinn, P. S. Zory, Jr., and A. R. Reisinger, IEEE J. Quantum Electron. **QE-24**, 2191 (1988).

[5]J. Z. Wilcox, G. L. Peterson, S. Ou, J. J. Yang, M. Jansen, and D. Schechter, J. Appl. Phys. **64**, 6564 (1988).

[6]H. Kressel and J. K. Butler, *Semiconductor Lasers and Heterojunction LEDs* (Academic, New York, 1977), pp. 459–461.

[7]A. R. Reisinger, P. S. Zory, Jr., and R. G. Waters, IEEE J. Quantum Electron. **QE-23**, 993 (1987).

[8]H. C. Casey, Jr. and M. B. Panish, *Heterostructure Lasers Part A: Fundamentals* (Academic, Orlando, FL, 1978), pp. 180 and 181.

[9]D. P. Bour, D. B. Gilbert, L. Elbaum, and M. G. Harvey, Appl. Phys. Lett. **53**, 2371 (1989).

[10]S. H. Pan, H. Shen, Z. Hang, F. H. Pollack, W. Zhuang, Q. Xu, A. P. Roth, R. A. Masut, C. Lacelle, and D. Morris, Phys. Rev. B **38**, 3375 (1988).

Downloaded 13 Mar 2013 to 129.25.131.13. Redistribution subject to AIP license or copyright; see http://jap.aip.org/about/rights_and_permissions